Scientific Research Publishing

Engineering, 2023, 15, 581-595
https://www.scirp.org/journal/eng
ISSN Online: 1947-394X
ISSN Print: 1947-3931

Multistage Triaxial Behavior of Shallow Landslide Hazard Site Soil of Rangamati Sadar Area, Bangladesh

Mahmuda Khatun*, Abu Taher Mohammad Shakhawat Hossain, Hossain Md. Sayem

Department of Geological Sciences, Jahangirnagar University, Dhaka, Bangladesh
Email: *mahmuda@juniv.edu

How to cite this paper: Khatun, M., Hossain, A.T.M.S. and Sayem, H.Md. (2023) Multistage Triaxial Behavior of Shallow Landslide Hazard Site Soil of Rangamati Sadar Area, Bangladesh. *Engineering*, **15**, 581-595.
https://doi.org/10.4236/eng.2023.1510041

Received: September 5, 2023
Accepted: October 17, 2023
Published: October 20, 2023

Abstract

The soil samples were collected from a shallow landslide hazard site of the Rangamati Sadar in Bangladesh to determine the shear strength properties of the soil. Multistage triaxial consolidation undrained test has become worldwide more accepted to determine the shear strength parameters. Multistage triaxial undrained tests were performed on five samples taken from five different depths of boreholes. Samples were evaluated under two natural conditions and three remolded situations. Samples were consolidated before shearing at confining pressures from 50 kPa to 1200 kPa. All the test results are discussed in terms of deviator stress versus axial strain, mean effective stress versus deviator curves, stress ratio versus axial strain, and excess p. w. p. versus axial strain curves. The samples consolidated at low effective stress first displayed peak positive values of excess p. w. p., followed by increased strains due to sample bulging failure, and only a few samples formed a shear surface failure. The strength parameters were estimated using the maximum deviator stress as the failure criterion *i.e.* the overall value of the cohesion is 20 kPa and the friction angle is 34˚. Hence, the critical state line has been constructed and the critical state parameters have been calculated. The critical state stress ratio M was calculated to be 0.036. The shear strength of soil is one of the significant mechanical properties that are thoroughly used to assess the landslide and liquefaction potentiality of the soil.

Keywords

Multistage Triaxial, Shear Strength, Critical State, Stress Path, Landslide

1. Introduction

The research area Rangamati Sadar, a southeastern folded part of Bangladesh is part of a hilly terrain where landslides have occurred frequently. It is very im-

portant to determine the soil property *i.e.*, shear strength the stability of slopes, retaining walls, and foundations. The triaxial test is the most commonly used laboratory equipment for studying soil strength and deformation behavior. In conventional tests, each specimen goes through a consolidation and shearing phase, resulting in a single stress vs. strain trend and, only one level of stress at failure.

The multi-stage triaxial tests, which use one specimen to determine its strengths under several different stages of confining stresses, appear to be an attractive alternative for the geomechanical characterization of shallow landslide site soil samples. In a multi-stage triaxial test, the specimen is clipped up to a shearing termination point under an initial confining pressure and then reconsolidated under a higher confining pressure for the next shear stage. This process is repeated multiple times to obtain soil strength under various confining stresses. The multi-stage triaxial test is an information-rich testing technique that utilizes a minimum number of specimens and can circumvent the consequences of the variability of specimens often observed from one single-stage triaxial test to the other [1]. Since its first practical application in the early 1950s [2], multi-stage triaxial tests have been successfully used to characterize the strength of various rocks and soils [3]-[8].

Authors [9] performed MCU (multistage undrained testing) that specifies reasonable consistency between the data acquired from MCU tests and those obtained from conventional undrained tests (CCU).

Although various research [1] [2] [10] [11] [12] [13] have demonstrated the economic viability of doing multistage triaxial testing on saturated soils, they have also identified the shear strength or effective shear strength of saturated as well as unsaturated soils [1] [10] [12] [14] and reviewed the test [13]. Consolidated undrained triaxial tests on various clay specimens using both conventional and multistage approaches and found that multistage compression tests concurred well with those conducted by [12].

Multistage triaxial tests can collect the most information from a small number of tests and reduce the effect of soil variability from one test to the next. The test results are easily applicable to soil slope stability and earth pressure problems.

It is important to understand the geotechnical properties and shear strength behavior on those properties and the associated difficulties related to the strength of this soil. This study intends to investigate the effect of engineering geological & geomechanical factors on landslides within the Rangamati Sadar area, Bangladesh. The main objective of this research work is to determine the subsurface condition and shear strength parameters of soils. The results will contribute to a better understanding of the nature of landslide occurrences *i.e.*, slope stability of the area.

2. Methodology

2.1. Multistage Procedure

A multistage test involves more than one consolidation and shearing on the

same soil specimen loaded inside a direct shear box. During the saturation stage of a triaxial test, it takes around 5 days to get a value of B (pore pressure) greater than 0.9 and complete the settling in this process. This strategy achieves significant homogeneity of outcomes while taking a significant amount of time. After the saturated and consolidated specimen in stage I is finished, the specimen is sheared to produce a large amount of shear stress. The specimen is then freed from stress. The specimen is subjected to higher normal stress before the shearing stage to begin the next stage.

The test procedure for the multi-stage undrained compression test used consisted of consolidating a sample under various cell pressures (at a range of effective confining pressures from 50 kPa up to 1200 kPa), computing the height and volume of the sample after each consolidation phase, increasing both the cell pressure and the pore pressure by equal amounts to dissolve any free air, and loading the sample until fail or brittle was reached. The overall strain applied to the sample during the MCU test was approximately 25%. All the samples carried out on strain rates of 0.002%/min to 0.005%/min for different types of soil by [13] [15] [16] [17] used a strain rate of 0.002%/min in their multistage testing on silty clayey soils. Any undrained test was finished, the load was taken out of the sample, and the pore pressure was allowed to stabilize for some time before the test was continued or the sample was taken out (**Figure 1**).

2.2. Triaxial Test Sample

Light cable percussion drilling was used to collect the samples. Undisturbed soil samples were collected with thin wall open Shelby tubes (U100) and disturbed samples were collected using a split spoon sampler. Natural samples were properly trimmed before each test. Cylindrical test specimens of length 76 mm. and diameter 38 mm. were prepared vertically from the central core part of the U100 tube. The test samples are described in **Table 1** and the index data of some of the samples are in **Table 2**.

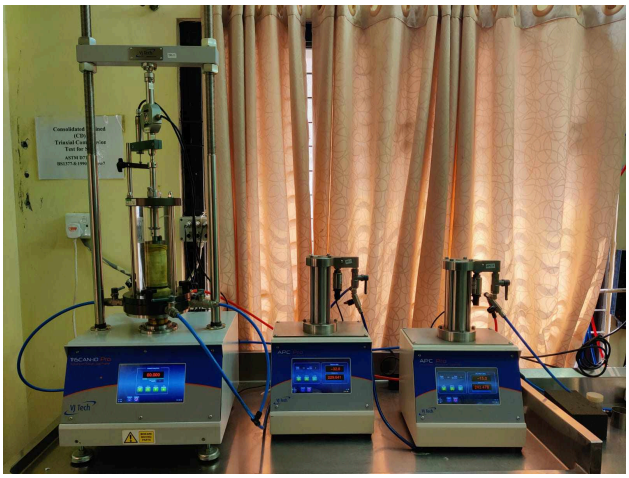

Figure 1. Consolidated Undrained Triaxial apparatus under test in laboratory ground instrumentation & engineering Pte Ltd, Singapore.

Table 1. Summary of basic geotechnical properties.

Location	Sample No	Depth (m)	Sand (%)	Silt + Clay (%)	Density (ϱ_s) Mg/m^3	Classification
Bangladesh Betar	BH1 S1	1.50 - 2.00	29.78	70.22	2.66	CL-MLS Silty Clay with Sand
Passport Office	BH2 S3	3.65 - 4.15	60.4	39.60	2.93	SMS Silty fine medium Sand
Gayye chara	BH4 S1	2.13 - 2.62	21.42	78.58	2.68	CL-MLS Silty Clay with Sand
C. M. B Ecopark	BH6 S2	2.13 - 2.62	80.84	19.16	2.70	SMS Silty fine medium Sand
Monoghar Playground	BH10 S1	0.90 - 1.40	51.38	48.62	2.57	SC-S Clayey fine medium dense Sand

Table 2. Undrained testing details different soils of Rangamati landslide sites.

Sample no.	Depth (m)	Initial Moisture content (%)	Particle density (ϱ_s) (Mg/m^3)	Bulk density ρ (Mg/m^3)	Initial Dry density ρ_d (Mg/m^3)	Dry density ρ_d (Mg/m^3)	Initial void ratio (e_0)	Wet weight of Sample (g)	Dry weight of the sample (g)
CU100	1.5 - 2.00	26	2.93	1.70	1.35	1.71	1.165	147.5	140.5
CU200	2.13 - 2.62	26	2.68	1.92	1.52	1.85	0.758	166.3	163.3
CU300	2.13 - 2.62	21	2.70	1.77	1.47	1.78	0.841	153.1	152.1
CU400	3.65 - 4.15	27	2.66	1.66	1.31	1.63	1.026	143.4	139.5
CU600	0.9 - 1.40	26	2.57	1.62	1.39	1.76	0.846	140.0	134.0

Consolidated undrained triaxial tests with pore water pressure measurements were carried out on the five undisturbed samples (Two natural Clay Samples *i.e.*, CD200 and CD400, and three remolded sand samples *i.e.*, CD100, CD300, and CD600) collected from several depths from a borehole in the Rangamati landslide-prone area of Bangladesh. The triaxial tests are conducted on the undisturbed soil specimens under consolidated undrained test with pore pressure measurement (CU) following the BS 1377-8: 1990 (7) [18] Standard Test Method at laboratory Ground Instrumentation & Engineering Pte Ltd in Singapore.

Before the tests, after placing and sealing the specimens inside the triaxial chamber and taking measurements of diameter and height, the soil specimens are saturated from the top until a value of B (the pore-water parameter) is 1.00 and it takes 4 - 5 days. For this purpose, the cell pressure and saturation water pressure (back pressure) are applied and increased gradually. A difference of 10 kPa between cell pressure and back pressure is maintained to prevent swelling or consolidation during saturation. After completing the saturation process, the soil specimens are consolidated under a confining pressure of σ_3, and pore water is allowed to drain out. Samples were consolidated for up to 24 hours at a range of confining pressures from 50 kPa up to 1200 kPa before shearing. The undrained compression stage was carried out at a constant rate of up to 20% strain.

Figure 2 shows different types of failure as bulging and Shear surface failure due to effective confining pressure. Samples are named by using letters and numbers. Two letters are used to designate each test. The first and second letters in each test indicate the type of shearing (consolidated undrained) and the number indicates the load applied to it, tested remolded state, which was consolidated at a confining pressure of 50 kPa before shearing. Remolded samples were prepared from the natural soils of the three boreholes and reformed with the same void ratio and dry density as the natural samples.

A single soil sample is subjected to three stages of confining pressures equivalent to 50, 100, and 200 kPa in the multi-stage triaxial (MST) compression test. The multi-stage triaxial compression test (MST) is an alternate method that requires only one soil specimen to be evaluated at three stages of shearing with various confining pressures as opposed to the usual three soil specimens used in traditional triaxial compression tests (CTC) approaches by [9] [10]. In addition to requiring fewer soil samples than CTC, adopting MST also saves time in the lab and minimizes the impact of heterogeneity on the specimens being evaluated. The fundamental benefit of a multi-stage triaxial test over a typical triaxial test is that it can provide accurate shear strength values without raising the related laboratory costs.

3. Results and Discussions

The landslide hazard site sample's basic geotechnical properties and testing details are shown in Table 1 and Table 2. The next sections follow details about multistage stress-strain curves, excess pore water pressure vs. axial strain, stress ratio, and stress path curves.

3.1. Stress-Strain Curves

The deviator stress (q) versus axial strain (ε %) curves under different confining pressures for all the samples are shown in Figure 3. It can be seen that the stress-strain curves show a maximum stress level in each case. The deviator stress increases with increasing the axial strain until the maximum value is reached (*i.e.*, peak point). In general, the deviator stress of most of the samples

(a) (b)

Figure 2. Failure nature—(a) Bulging and (b) Shear in Triaxial Consolidated Undrained test.

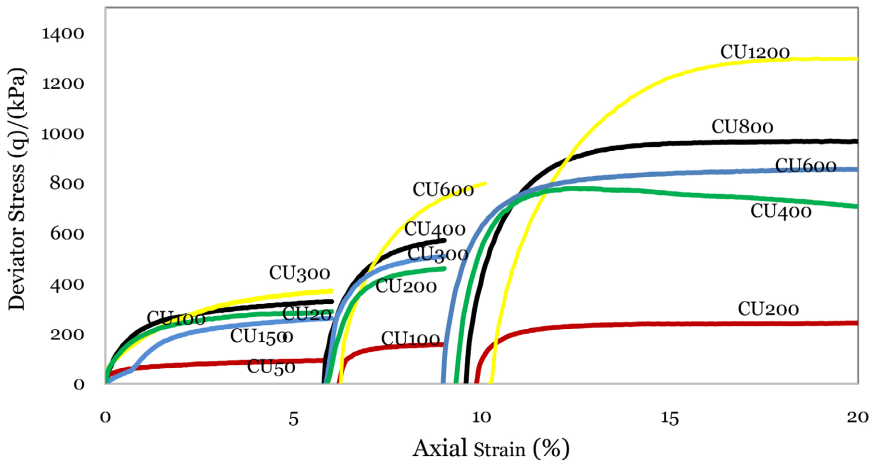

Figure 3. Deviator stress versus axial strain curves of different depth soil samples.

dropped off significantly immediately after peaking in stage III. The samples seemed to show signs of failure in the third stage of loading. The drop in strength in stage III appeared to be related to the amount of strain accumulated while samples were failing. It is suggested that the specimen should not be deformed excessively during the earlier stage of loading (past peak strength). The peak values of q for samples consolidated to effective pressures of 1200 kPa or more have a more prominent peak than those consolidated to lower stresses. It can also be seen from this figure that the maximum deviator stress increases with increasing effective consolidation pressure.

The axial strains to attain maximum deviator stress for these samples range from 6% to 20%. The maximum deviator stress and the corresponding values of axial strain, mean effective stress, and excess pore water in each case are summarized in Table 3.

3.2. Excess Pore Water Pressure versus Strain Curves

The excess pore water pressures (p. w. p.) versus strain curves for all samples are shown in Figure 4. The excess pore water pressure increases initially, reaches a peak, and then decreases with increasing strain. Tests at low confining pressure (50 to 300 kPa) initially showed low values of positive pore water pressures, followed by higher axial strains. All the samples had no negative pore pressure at higher confining pressures. Generally, most of the tested samples show normal behavior during the shearing process, indicating the behavior of normal to lightly over-consolidated soil. The test results also indicate that the confining pressure (σ_3) has an important role in the variation of pore water pressure during loading so that excess pore water pressure increases as confining pressure increases.

The graph of excess pore water pressure vs. axial strain (Figure 4) reveals a general trend between excess p. w. p. and confining pressure. In all samples, the maximum positive excess pore water pressure values lie between approximately

7 kPa to 321 kPa. The highest value of positive excess p. w. p. is for sample BH-4 (S1) of effective pressure CU400, whereas the lowest value was for sample BH-6 (S2) of effective pressure CU150. Table 3 shows the highest deviator stress in each state. These values lie in the 150 kPa to 400 kPa range from stage I to stage III. In all samples, excess pore water pressures have reached their maximum values at lower axial strains than that of the maximum deviator stress.

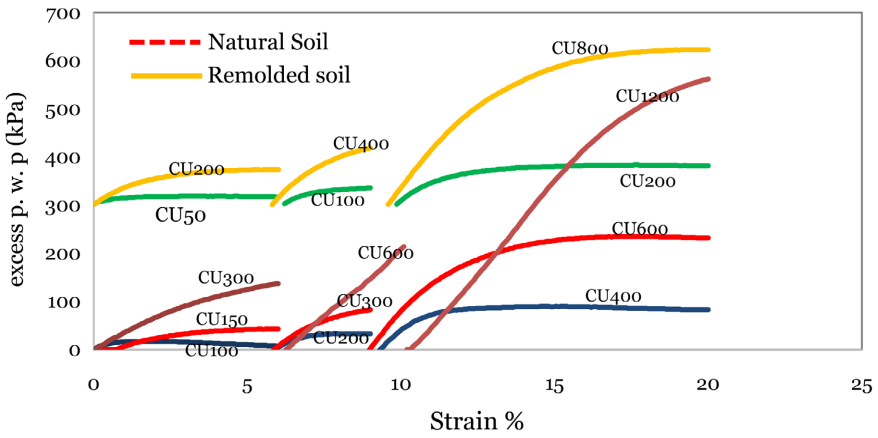

Figure 4. Excess pore water pressure versus axial strain curve of different depth soil samples.

Table 3. Summary of stress and strain parameters at maximum deviator stress.

Sample No	Stage	Max deviator stress (q) kPa	Excess p. w. p. at max q(u) kPa	Axial strain at max q (ε, %)	Mean effective stress (p') at max kPa
CU50	I	93.3	15	6	72.2
CU100	II	155.7	33	9	136
CU200	III	242	80	20	231.1
CU100	I	327.4	73	6	283.8
CU200	II	570.8	118	9	560.7
CU400	III	965.1	321	20	952.7
CU150	I	287	7	6	231.1
CU300	II	458.8	33	9	386.5
CU600	III	706.6	83	20	660.3
CU200	I	260.6	43	6	232.2
CU400	II	507.2	83	9	464.7
CU800	III	853.2	232	20	788.4
CU300	I	369.4	137	6	341.9
CU600	II	798.5	214	10.9	779.2
CU1200	III	1293.5	297	20	1277.3

By comparing the excess p. w. p. and strain curves, it is evident that samples at low effective consolidation pressures, 50 to 300 kPa, showed a continuous change of p. w. p. up to the end of the test and therefore, these samples have not reached a steady state at the end of shearing. If it has been possible to continue shearing at more than 20% strain, it might be possible that these samples might have reached the steady state as they did not form distinct shear surfaces.

It can be seen from **Figure 4** that the excess p. w. p. for tests all the samples tended towards constant values at very large strains (approximately over 20% strains) except CU300, which indicates that they are approaching the critical state. However, these two samples formed distinct shear surfaces. It is therefore difficult to justify that these samples have truly reached the critical state. Other can be seen in cohesive samples from **Figure 4**, at low to medium effective consolidation pressures (CU50, CU100, and CU150) seem to be constant at stage III until the end of the test and they also formed a bulging failure. Therefore, these samples also have reached the critical state at the end of shearing. In all samples, excess pore water pressures have reached their maximum values at higher axial strains on stage III than the point at which maximum deviator stress occurred (**Figure 4**).

3.3. Stress Ratio (q/p') vs. Strain Curves

[19] Pointed out that the maximum stress ratio (q/p') value does not necessarily occur at the same strain as the peak deviator stress. The maximum stress ratio criterion is preferable to the peak stress ratio criterion in some ways because it can provide a better correlation of shear strength with other parameters, or between different types of tests. It is particularly useful for clays in which the deviator stress continues to increase at larger strains. [20] Mentioned that soils are frictional materials and their strength increases with normal stress so the stress ratio is more important than the shear stress alone. The maximum q/p ratio versus strain graphs is shown in **Figure 5**. The maximum q/p ratios occurred at strains from 3.99% to 8.97%.

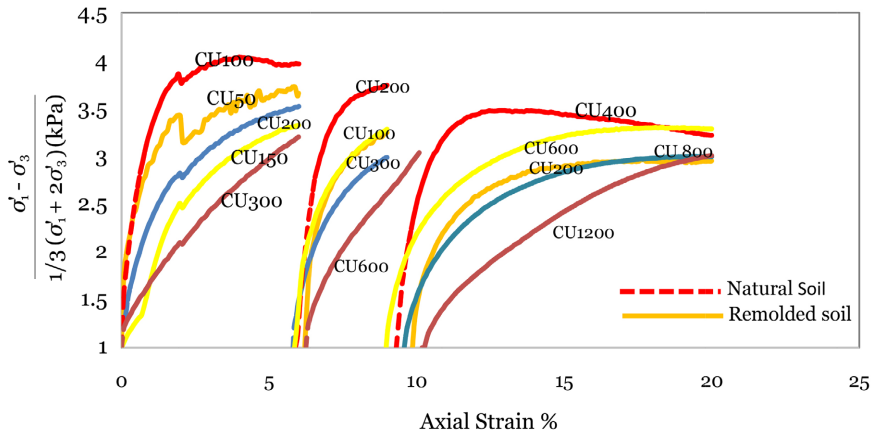

Figure 5. q/p' ratio versus strain (%) curves of different depths of soils.

The maximum q/p values for these samples lie from 1 to 4.02. The highest and lowest maximum stress ratio values for these samples are observed in tests CU100 and CU150 respectively. After reaching the maximum q/p values at 6% strains, some of the samples reached a constant stress ratio state at strains greater than 20% (Figure 5). After reaching the maximum q/p' values at low strains (Stage I) all samples showed a tendency to drop continuously to strain 9% strain. At stage III maximum soils reached a constant stress ratio state except for CU1200 (Figure 5). A variation in the maximum q/p ratio value is observed with the increase of effective confining pressures for these samples. In general, low effective consolidation pressure (Stage I) samples showed higher values of maximum q/p ratio value than the high effective consolidation pressure samples.

3.4. Effective Stress Paths in q - p'

The effective stress paths for all the samples (both natural and remolded) under different confining pressures are shown in Figure 6. The stress paths are drowned in the (p' - q') plane using the Cambridge stress system, p' is the mean effective stress q' is the deviator stress, σ'_1 is a major principle effective stress and σ'_3 is a minor principle effective stress. The stress paths at low effective consolidation pressures, 50 to 200 kPa, (Figure 6) initially increased a straight line and then showed a tendency to move towards the left. At higher effective consolidation pressures, 400 to 1200 kPa, each stress path at the beginning of each test, shows a tendency to move towards the left with an increase of deviator stress. A clear change of behavior can also be observed in the excess p. w. p. versus strain curves as shown in Figure 4.

With the increase of p and q', each stress path shows a tendency to move towards the left when they are approaching failure. After reaching the failure zone, the stress paths curve starts to down (possibly approaching the critical state line, CSL). The values of mean effective stress at maximum deviator stress and the

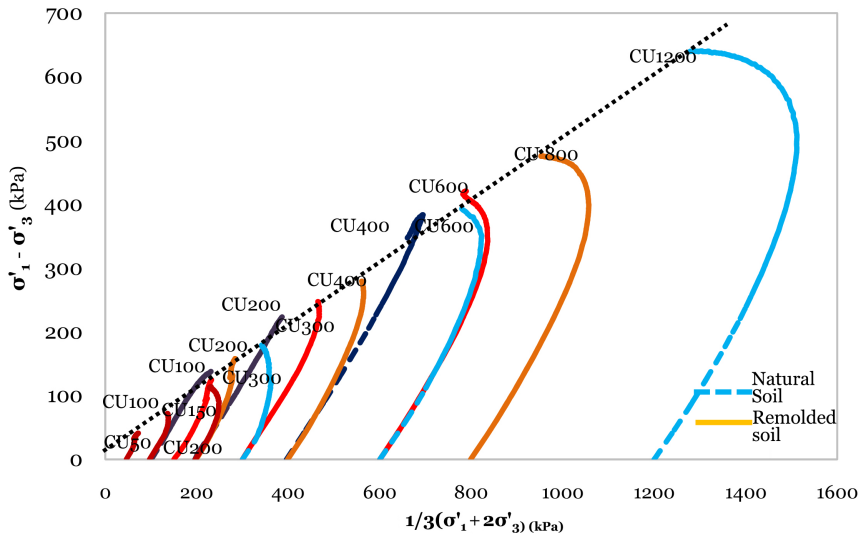

Figure 6. Effective stress paths of different depth soil samples.

corresponding maximum deviator stress for these stress paths are mentioned in Table 3. The failure points and end points are almost close to each other for most of the samples. It is found in Figure 6 that the mean effective stress values at failure increase with increasing confining pressure. Consequently, the deviator stress at failure also increases with the increase of mean effective stress (Figure 6). Figure 6 describes the shear stress and pore water pressure curves as a function of shear duration for various normal stresses. In this research, the void ratio is considered a weathering process function and is unrelated to stress history.

3.5. Failure Surface of Soils

A failure envelope in terms of effective stress for a set of tests is plotted in the $q - p'$ space, as shown in Figure 7. It shows a linear failure envelope. All the lower confining pressure samples failed with the formation of shear planes. At low effective consolidation pressures sample BH4/S1 (100 kPa), the shear planes were distinct. Samples CU100, CU300, and CU400 failed with several indistinct shear planes with bulging failure. Two samples also failed with distinct shear planes. However, at high effective consolidation pressures, in samples CU400 to CU600, shear planes were more prominent and distinct and the samples failed along a distinct single shear plane. Similar distinct polished shear planes were observed by [21] on London Clay. The failure surface for the whole range of tests for these soils showed a linear up to approximately p' = 1200 kPa. The slope of the curve reduces steadily as p' increases and samples reach a maximum q/p' ratio before failure followed by a decrease with increasing strain to the end of the test. From the failure envelope, shear strength Parameters are Cohesion (c) values of 20 (kPa), and a Friction Angle (φ) of 34˚ was obtained. The obtained value is very close to the author's [9] [22].

3.6. Critical State Behaviour

Finally, based on the experimental results the critical state parameters for these soils have been calculated and shown in Figure 8.

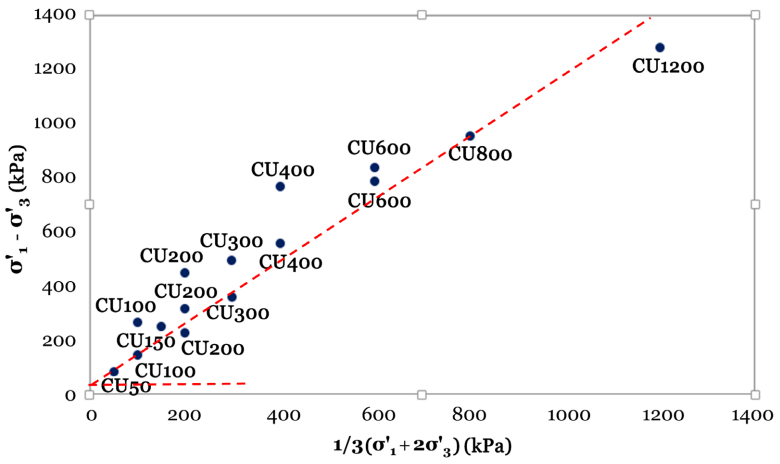

Figure 7. Failure surface of different depth soil samples.

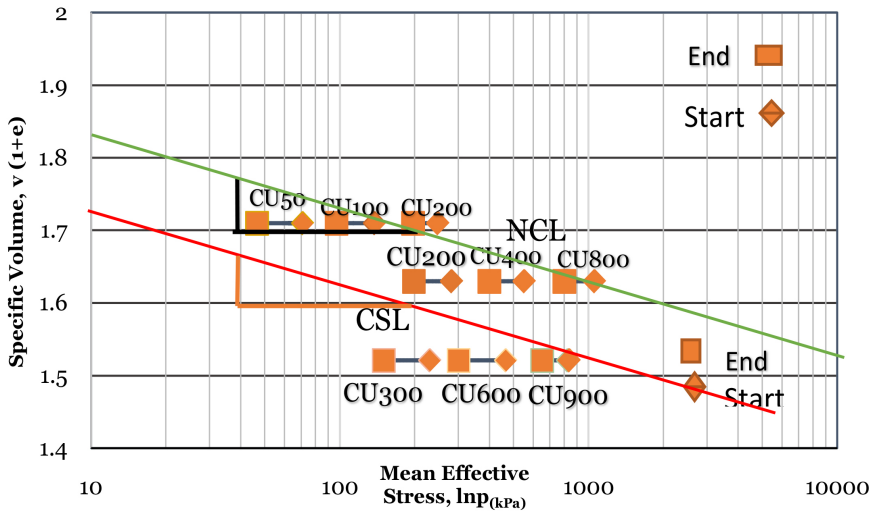

Figure 8. Specific volume versus p' for different depth soil samples.

[20] [23] mentioned that the intrinsic critical state parameters (M, λ, and τ) depend principally on the nature of the soil and might vary due to differences in grading and mineralogy from sample to sample.

From the q/p ratio versus strain graphs (**Figure 6**) it was difficult to identify a single common ultimate stress ratio value for these soils. The values of the maximum q/p ratio showed a range of variations. The maximum q/p values obtained in between 1 to 4.02. It is interesting to see that all samples at low effective consolidation pressures (50, 100, and 300 kPa) have a similar ultimate stress value of around 1. It is important to note here that these low confining pressure samples did not form distinct shear surfaces; therefore, the ultimate stress ratio for these tests might represent the critical state. A true critical state was not achieved for these low-stress tests, as pore water pressure continued to change even at large strains when the tests were terminated. However, most of the low-stress tests showed that the rate of decrease of pore water pressure reduced towards the end of the test and they did not form distinct shear planes indicating that the critical state was being approached. All the samples at stages I & II did not develop shear surfaces but in stage III at higher strain maximum samples developed bulging shapes and few samples developed distinct shear surfaces.

On the other hand, samples at high confining pressures fail along distinct shear in a narrow band and the "overall" stress ratio and volume change are no longer representative of the sample as a whole. It is difficult to justify that these samples have truly reached a critical state. This makes it difficult to construct a single unique CSL for these soils. [24] mentioned a value of M = 1.73 for the river sand and noted that few intact samples of Rangamati soil reached reasonably well-defined constant ratio states at very large strains.

All the undrained results of natural soils are also presented in the v (specific volume) versus p space to see the change of specific volume with increasing mean effective stress. These results are also evaluated in terms of the critical state. The v versus p curves for these soils are shown in **Figure 8**. By considering

the starting and end points of each test it is difficult to construct a single critical state line for these samples. However, if the greatest consideration is given to the low-stress tests, up to 300 kPa, where it was observed that failure did not involve a single distinct shear plane, a trend in terms of changes in mean effective stress (p) can be seen. This suggests that the CSL would fall between the endpoints for these four tests. Again, from **Figure 6**, it can also be seen that these soils at low effective consolidation pressures (50 to 200 kPa) also moved to the left except CU100 kPa moved left to the right side with almost a constant specific volume. However, the stress ratio value varies in all samples from 1 m to 4.02 m, consolidated between 50 to 300 kPa, and might represent the critical state as they do not form distinct shear surfaces. These are the difficulties in defining the critical state of this fine to medium loose sand.

On the other hand, the high effective consolidation pressure, samples 400 to 600 kPa, initially moved towards the assumed critical state line due to a tendency to contract that produces positive pore water pressures. They moved towards the assumed critical state line with a lower specific volume. The tests at 400 - 800 kPa (**Figure 8**) show an overall movement of an increase in p, even though they are above the apparent CSL. This is probably due to the formation of distinct shear planes in these tests. Initially, they do show a decrease in p consistent with the sketched CSL. The change in direction may represent the initiation of a distinct shear surface when the pore water pressures measured no longer indicate what is happening within the failure surface itself. However, as these soils at high confining pressures also formed distinct shear surfaces, it is difficult to establish with confidence that these samples truly reached the critical state at very large strains. It is, therefore, logical to consider only low-stress tests (50 - 300 kPa) in defining critical state lines.

[20] Pointed out that the critical state parameters for a particular soil are generally considered to be constant. The variation seen in the stress ratio values and also difficulties in defining the CSL from v versus p' curves made it difficult to obtain typical critical state parameters for these soils. However, based on all observed results on tested soils a rough estimation was made to obtain the critical state parameters for the sandy soils of Rangamati. The intrinsic critical state parameters critical state friction constant, M, isotropic normal compression line, and an ordinate critical state line are shown and compared with the other values as quoted by [20] in **Table 4**.

Table 4. Comparison obtained critical state parameters of Rangamati soil with some typical soils [24] [25] [26].

Soil	λ	Γ	M
London Clay	0.16	2.45	0.89
Tropical clay, Dhaka	0.06	1.83	0.95 - 0.96
River Sand (Coarse-grained)	0.16	2.99	1.28
Balukhali Soil	1.6	1.8	0.32
Rangamati Soil (Medium to fine Sand)	0.046	1.73	1.84

4. Conclusions

This research dealt with the behavior of the shallow landslide hazard site soil samples of the investigated area, including the different geomechanical parameters of the soil. Multistage undrained triaxial tests were carried out on samples collected from five boreholes in the landslide-prone area of the Rangamati Sadar area. In undrained shearing at low confining pressure, samples showed positive values of excess p. w. p. followed by higher strains in all the samples. No negative pore water pressure was observed for those samples consolidated at higher effective stress. The samples showed a wide range of ultimate stress ratio values at strains from 3.90% to 8.97%. The effective stress path showed with increasing effective consolidation pressure each stress path tends to move towards the left when they are approaching failure. As the failure points and end points are very close to each other, it also indicates the strengthening behavior of the soil. The obtained cohesion value is 20 kPa and the friction angle is 34˚. The specimen did not form shear surfaces during stages I & II of low stress whereas in stage III at higher strain most samples develop bulging shapes and only a small number of samples produce distinct shear surfaces. The v-log p' curve, the critical state line (CSL), and the Normal consolidation line (NCL) are drawn as well as the critical state parameters have been calculated where are $-\lambda = 0.043$, $\Gamma = 1.73$, and $M = 1.84$ were estimated under undrained shearing. However, as there are difficulties in defining one critical state condition for these soils, these values probably only represent the shallower samples.

The evaluation of triaxial shear strength parameters to evaluate the landslide potentiality is extremely important to assess the risk and community living in the study area.

This time benefiting research project has been taken to evaluate the hazards evaluation from the geomechanical point of view to mitigate the hazard in the study area, protect landslide-affected people, and build up different engineering structures safely and economically.

Acknowledgements

This paper is a part of the first author Mahmuda Khatun's Ph.D. Research work at the Department of Geological Sciences, Jahangirnagar University, Savar, Dhaka, Bangladesh. The authors sincerely thank Ground Instrumentation & Engineering Pte Ltd, Singapore laboratory for carrying out the research.

Conflicts of Interest

The authors declare no conflicts of interest regarding the publication of this paper.

References

[1] Ho, D.Y.F. and Fredlund, D.G. (1982) A Multistage Triaxial Test for Unsaturated Soil. *Geotechnical Testing Journal*, **5**, 18-25. https://doi.org/10.1520/GTJ10795J

[2] Taylor, D.W. (1951) A Triaxial Shear Investigation on a Partially Saturated Soil. In: *Triaxial Testing of Soils and Bituminous Mixtures*, ASTM International, Philadelphia, 180-191. https://doi.org/10.1520/STP48414S

[3] Goodman, R. (1974) The Mechanical Properties of Joints. *Proceedings of the Third International Congress International Society of Rock Mechanics*, Denver, 1-7 September 1974, 127-140.

[4] Houston, S.L., Perez-Garcia, N. and Houston, W.N. (2008) Shear Strength and Shear-Induced Volume Change Behavior of Unsaturated Soils from a Triaxial Test Program. *Journal of geotechnical and Geoenvironmental Engineering*, **134**, 1619-1632. https://doi.org/10.1061/(ASCE)1090-0241(2008)134:11(1619)

[5] Kovari, K. and Tisa, A. (1975) Multiple Failure State and Strain Controlled Triaxial Tests. *Rock Mechanics*, **7**, 17-33. https://doi.org/10.1007/BF01239232

[6] Mishra, B. and Verma, P. (2015) Uniaxial and Triaxial Single and Multistage Creep Tests on Coal-Measure Shale Rocks. *International Journal of Coal Geology*, **137**, 55-65. https://doi.org/10.1016/j.coal.2014.11.005

[7] Parker, J., Amos, D. and Sture, S. (1980) Measurement of Swelling, Hydraulic Conductivity, and Shear Strength in a Multistage Triaxial Test. *Soil Science Society of America Journal*, **44**, 1133-1138. https://doi.org/10.2136/sssaj1980.03615995004400060002x

[8] Youn, H. and Tonon, F. (2010) Multi-Stage Triaxial Test on Brittle Rock. *International Journal of Rock Mechanics and Mining Sciences*, **47**, 678-684. https://doi.org/10.1016/j.ijrmms.2009.12.017

[9] Kenny, T.C. and Watson, G.H. (1961) Multi-Stage Triaxial Test for Determining c' and f' of Saturated Soils. *Proceedings of the 5th International Conference on Soil Mechanics and Foundation Engineering*, Paris, 17-22 July 1961, 191-195.

[10] De Beer, E.E. (1950) The Cell Test. *Geotechnique*, **2**, 162-172. https://doi.org/10.1680/geot.1950.2.2.162

[11] Saeedy, H.S. and Mollah, M.A. (1988) Application of Multi-Stage Triaxial Test to Kuwaiti Soils. In: Donaghe, R.T., Chaney, R.C. and Silver, M.L., Eds., *Advanced Triaxial Testing of Soil and Rock*, ASTM, Philadelphia, 363-375. https://doi.org/10.1520/STP29087S

[12] Soranzo, M. (1988) Results and Interpretation of Multistage Triaxial Compression Tests. In: Donaghe, R.T., Chaney, R.C. and Silver, M.L., Eds., *Advanced Triaxial Testing of Soil and Rock*, ASTM, Philadelphia, 353-362. https://doi.org/10.1520/STP29086S

[13] Hormdee, D., Kaikeerati, N. and Angsuwotai, P. (2012) Evaluation on the Results of Multistage Shear Test. *International Journal of GEOMATE*, **2**, 140-143.

[14] Anderson, W.F. (1974) The Use of Multi-Stage Triaxial Tests to Find the Undrained Strength Parameters of Stony Boulder Clay. *Proceedings of the Institution of Civil Engineers*, **57**, 367-373. https://doi.org/10.1680/iicep.1974.4063

[15] Sharma, M.S.R., Baxter, C.D.P., Hoffmann, W., Moran, K. and Vaziri, H. (2011) Characterization of Weakly Cemented Sands Using Nonlinear Failure Envelopes. *International Journal of Rock Mechanics and Mining Sciences*, **48**, 146-151.

[16] Sridharan, A. and Narasimha Rao, S. (1972) New Approach to Multistage Triaxial Test. *Journal of Soil Mechanics and Foundation Division*, **98**, 1279-1286. https://doi.org/10.1061/JSFEAQ.0001813

[17] Kondner, R.L. (1963) Hyperbolic Stress-Strain Response: Cohesive Soils. *Journal of Soil Mechanics and Foundation Division*, **89**, 115-143. https://doi.org/10.1061/JSFEAQ.0000479

[18] British Standard 1377 (1990) Methods for Test for Civil Engineering Purposes. British Standard Institution, London.

[19] Head, K.H. (1986) Manual of Laboratory Testing. Pentech Press, London.

[20] Atkinson, J.H. (1993) Introduction to the Mechanics of Soils and Foundations. McGraw Hill International Series in Civil Engineering, London.

[21] Jardine, R.J., Symes, M.J. and Urland, J.B. (1984) The Measurement of Soil Stiffness in the Triaxial Apparatus. *Geotechnique*, **34**, 323-340. https://doi.org/10.1680/geot.1984.34.3.323

[22] Nambiar, M.R.M., Rao, G.V. and Gulhati, K.S. (1985) Multistage Triaxial Testing: A Rational Procedure. In: Chaney, R.C. and Demars, K.R., Eds., *Strength Testing of Marine Sediments*: *Laboratory and in-situ Measurements*, American Society for Testing and Materials, Philadelphia, 274-293. https://doi.org/10.1520/STP36340S

[23] Hossain, A.T.M.S. (2001) The Engineering Behavior of Tropical Madhupur Clay Soil of Dhaka, Bangladesh. Ph.D. Thesis, University of Durham, Durham.

[24] Allman, M.A. and Atkinson, J.H. (1992) Mechanical Properties of Reconstituted Bothkennar Soil. *Géotechnique*, **42**, 289-301. https://doi.org/10.1680/geot.1992.42.2.289

[25] Hossain, A.T.M.S. and Toll, D.G. (2012) Geotechnical Behaviour of Unsaturated Tropical Clay Soils of Dhaka, Bangladesh. In: Mancuso, C., Jommi, C. and D'Onza, F., Eds., *Unsaturated Soils*: *Research and Applications*, Springer, Berlin, 309-316. https://doi.org/10.1007/978-3-642-31116-1_42

[26] Sheikh, J.J. (2023) Rainfall Induced Landslide Risk Assessment at Balukhali Rohingya Refugee Camp Area, Ukhiya, Cox's Bazar, Bangladesh—A Geotechnical Engineering Approach. Master's Thesis, Jahangirnagar University, Dhaka.